

BIROn - Birkbeck Institutional Research Online

Chen, S. and Glasauer, S. and Muller, Hermann and Conci, M. (2018) Surface filling-in and contour interpolation contribute independently to Kanizsa figure formation. *Journal of Experimental Psychology: Human Perception and Performance* 44 (9), pp. 1399-1413. ISSN 0096-1523.

Downloaded from: <https://eprints.bbk.ac.uk/id/eprint/27058/>

Usage Guidelines:

Please refer to usage guidelines at <https://eprints.bbk.ac.uk/policies.html>
contact lib-eprints@bbk.ac.uk.

or alternatively

1

2

3

Surface filling-in and contour interpolation contribute independently to

4

Kanizsa figure formation

5

6

Siyi Chen, Stefan Glasauer, Hermann J. Müller, Markus Conci

7

Ludwig-Maximilians-Universität München, Germany

8

9

10

Running Head: Filling-in and contour interpolation in Kanizsa figures

11

Word count: main text: 8490, abstract: 200, significance statement: 146

12

13

14

Correspondence:

15

Siyi Chen

16

Allgemeine und Experimentelle Psychologie

17

Department Psychologie

18

Ludwig-Maximilians-Universität

19

Leopoldstr. 13

20

D-80802 München

21

Germany

22

Email: Siyi.Chen@psy.lmu.de

23

24 **Abstract (200)**

25 To explore mechanisms of object integration, the present experiments examined
26 how completion of illusory contours and surfaces modulates the sensitivity of
27 localizing a target probe. Observers had to judge whether a briefly presented dot
28 probe was located inside or outside the region demarcated by inducer elements that
29 grouped to form variants of an illusory, Kanizsa-type figure. From the resulting
30 psychometric functions, we determined observers' discrimination thresholds as a
31 sensitivity measure. Experiment 1 showed that sensitivity was systematically
32 modulated by the amount of surface and contour completion afforded by a given
33 configuration. Experiments 2 and 3 presented stimulus variants that induced an
34 (occluded) object without clearly defined bounding contours, which gave rise to a
35 relative sensitivity increase for surface variations on their own. Experiments 4 and 5
36 were performed to rule out that these performance modulations are simply attributable
37 to variable distances between critical local inducers, or to costs in processing an
38 interrupted contour. Collectively, the findings provide evidence for a dissociation
39 between surface and contour processing, supporting a model of object integration in
40 which completion is instantiated by feedforward processing that independently
41 renders surface filling-in and contour interpolation and a feedback loop that integrates
42 these outputs into a complete whole.

43

44 Keywords: Kanizsa figure, illusory contours, surface filling-in, modal completion,
45 amodal completion

46

47 **Public Significance Statement**

48 One of the fundamental operations of human vision concerns the identification of
49 relevant perceptual units, or objects that are present in the visual ambient array. A
50 prime example to demonstrate such mechanisms of object integration is the Kanizsa
51 figure, which illustrates that separate parts may be effectively bound to represent a
52 coherent whole. This study was performed to investigate complementary mechanisms
53 underlying object completion, namely the extraction of a bounding contour and its
54 concurrent estimation of the surface area in perceiving a coherent Kanizsa figure. In a
55 series of experiments, illusory figure sensitivity was measured using a dot-localization
56 task while contrasting the relative impact of contour and surface completion
57 mechanisms. We show that both contour and surface completions substantially impact
58 illusory figure sensitivity, but importantly, both processes of object completion appear
59 to operate relatively independent of each other, which has implications for models of
60 object integration.

61

62 **Introduction**

63 Detecting the boundaries of objects is a fundamental task of early vision, so as to
64 identify the available perceptual units, or objects, and segment these from other
65 objects and from the background (Cornsweet, 1970; Marr, 1982). In many situations,
66 object perception occurs despite degraded ambient luminance conditions, attesting to
67 a remarkable capability of the visual system to integrate separate fragments into
68 coherent wholes. This is illustrated in various examples of illusory figures (Kanizsa,
69 1955), where the presentation of ‘pacman’-type inducer elements gives rise to the
70 perception of illusory objects. For example, in Figure 1 (Kanizsa), a diamond-shape
71 object is perceived to occlude neighboring parts of four circular elements, despite
72 physically homogenous luminance across the diamond and background. Such a
73 perceptual ‘filling-in’ of an object, accompanied by a concurrent brightness
74 enhancement of the filled-in surface, is referred to as ‘modal completion’.

75 It is commonly assumed that the mechanisms underlying such completion
76 phenomena reflect the interpolation of the missing parts of the bounding contours and
77 the filling-in of the surface of the enclosed area (Grossberg & Mingolla, 1985; Pessoa,
78 Thompson, & Noë, 1998; Kogo, Strecha, Van Gool, & Wagemans, 2010). For
79 instance, results from neurophysiological recordings suggest that the filling-in process,
80 which generates the perception of an illusory surface, is associated with activations in
81 the lateral occipital complex (LOC) and the fusiform gyrus (e.g., Stanley & Rubin,
82 2003; Bakar, Liu, Conci, Elliott, & Ioannides, 2008), while boundary completion is
83 accomplished in both V1 and V2 (Lee & Nguyen, 2001; Von Der Heydt, Peterhans, &
84 Baurngartner, 1984) and to some extent also in the LOC (Shpaner, Stanley, Rubin, &
85 Foxe, 2004; Murray, Imber, Javitt, & Foxe, 2006). Together, these findings suggest
86 that separate regions in the ventral visual processing stream make distinct functional
87 contributions to the perception of illusory figures (Seghier & Vuilleumier, 2006, for a
88 review). The present study aimed at determining the relative contributions of such
89 contour and surface completion mechanisms in forming the percept of an illusory
90 figure.

91 Recent behavioral studies have used the visual search paradigm to systematically

92 examine the role of surface and contour processing in variations of Kanizsa figures.
93 To this end, configurations were generated that either presented an illusory Kanizsa
94 figure (Figure 1, Kanizsa), or a symmetric configuration that does not induce an
95 illusory shape (Figure 1, Baseline). Additional configurations induced ‘partial’
96 groupings, that is, either a partial illusory contour (Figure 1, Contour) or a partial
97 contour-plus-surface arrangement (Figure 1, Shape). Conci, Müller, and Elliott (2007a)
98 presented such configurations in a visual search task to investigate how surface and
99 contour grouping in distractors would modulate detection of a Kanizsa target shape.
100 They found that the partial surface, but not the presence of contours in distractors,
101 modulates the efficiency with which a Kanizsa target square is detected (see also
102 Conci, Gramann, Müller, & Elliott, 2006; Nie, Maurer, Müller, & Conci, 2016). This
103 suggests that the selection of an illusory figure primarily relies on processes of surface
104 filling-in. In this view, visual search with illusory figures is largely guided by a crude
105 specification of a closed target shape, without requirement to compute the exact
106 contours of the respective objects. However, the type of search task used in this study
107 (see Davis & Driver, 1994) likely only requires a relatively broad tuning of attention
108 to a target (Kanizsa) shape, so that it might, in fact, underestimate the role of contour
109 interpolation. By contrast, studies of neuropsychological patients with visual neglect
110 (Vuilleumier & Landis, 1998; Vuilleumier, Valenza, & Landis, 2001) indicate that
111 contour completion can also determine attentional selection, thereby reducing
112 extinction behavior. This suggests that both the filling-in of surfaces and the
113 interpolation of the bounding contours might be accomplished at early stages of visual
114 processing, thus guiding attention to potential target locations.

115 To directly measure illusory figure completion, Stanley and Rubin (2003) used
116 a psychophysical method that allows perceptual sensitivity to be determined in a
117 dot-localization task (see also Guttman & Kellman, 2004). The task involved the
118 localization of a dot probe, which was presented briefly near a presumed illusory edge
119 in a Kanizsa figure configuration. Observers were asked to decide whether the
120 presented dot appeared inside or outside the region demarcated by the Kanizsa figure.
121 Performance in this task was then used to determine psychometric functions, with

122 their slope parameter characterizing the dot-localization sensitivity. Stanley and Rubin
123 showed that the sensitivity in localizing the dot was significantly higher for an
124 illusory (Kanizsa) figure than for a configuration that presented a closed region
125 without concurrent illusory contour. Using a roughly similar method (but without
126 explicitly quantifying sensitivity), it has also been shown that detection of a target dot
127 is more efficient inside an illusory edge of a Kanizsa figure than outside (Ricciardelli,
128 Bonfiglioli, Nicoletti, & Umiltá, 2001). Together, these findings suggest that the
129 perceptual sensitivity in the dot-localization task can provide an indirect measure of
130 grouping strength, with the Kanizsa figure being associated with a higher sensitivity
131 than a comparable configuration without illusory object.

132 To further investigate how contours and surfaces influence the completion of
133 Kanizsa figures, the current study presented configurations that allow for a
134 dissociation of the respective surface and contour portions of a grouped figure (see
135 Conci et al., 2006; 2007a) using the dot-localization task (Stanley & Rubin, 2003) in a
136 series of psychophysical experiments. The configurations that were presented in the
137 experiments were characterized by a graded amount of surface and contour in variants
138 of Kanizsa figure configurations (see Figure 1): the Kanizsa diamond induces a
139 complete illusory figure (Figure 1, Kanizsa), the ‘Shape’ configuration provides
140 partial surface and contour information (Figure 1, Shape), and the ‘Contour’
141 configuration induces only a partial illusory contour (Figure 1, Contour); the
142 ‘Baseline’ arrangement, by contrast, presents no grouped object (i.e., no illusory
143 figure) while consisting of similar inducer elements and a symmetric arrangement
144 (Figure 1, Baseline). The efficiency of illusory figure completion was measured by
145 quantifying the discrimination in the inside/outside dot-localization task by
146 determining psychometric functions for these four types of configuration. The
147 discrimination threshold of the psychometric functions was then used as a measure of
148 the perceptual sensitivity. Thus, comparing the perceptual sensitivity among the
149 Kanizsa, Shape, Contour, and Baseline conditions permitted us to effectively assess
150 how contour interpolation and surface filling-in processes contribute to the
151 completion of an illusory figure.

152

153

Experiment 1

154

155

156

157

158

159

160

161

162

Experiment 1 was performed to measure the contribution of surface and contour completions in illusory figure perception, by employing a dot-localization task in which observers had to decide whether a target dot was located inside or outside a region demarcated by the inducer elements of a Kanizsa-type configuration (see also Stanley & Rubin, 2003, and Figure 1 for possible types of configuration). The discrimination threshold of dot-localization performance estimated from the psychometric function was taken as a measure of the perceptual sensitivity for a given configuration, thus permitting us to assess how surface filling-in and contour interpolation modulate the perceptual sensitivity.

163

Method

164

165

166

167

168

169

170

171

172

173

174

175

176

177

178

Participants. Twelve right-handed volunteers (8 men; mean age: 23.42 ± 1.98 years) with normal or corrected-to-normal visual acuity participated in the experiment for payment of €8.00 per hour. All participants provided written informed consent, and the experimental procedure was approved by the ethics committee of the Department of Psychology, Ludwig-Maximilians-Universität München. The sample size was determined on the basis of previous, comparable studies (e.g., Stanley & Rubin, 2003), aiming for 80% power to detect a relatively large effect size ($f=.4$; cf. Cohen, 1988) when using a repeated-measures ANOVA (within-factors, 4 conditions) with an alpha level of .05. Power estimates were computed using G*Power (Erdfelder, Faul, & Buchner, 1996). It should be noted that studies, which compute psychometric functions tend to conventionally test rather small samples, often with less than ten observers (e.g. Shi & Nijhawan, 2008; Hickok, Farahbod, & Saberi, 2015), but at the same time seek to thoroughly characterize performance for each subject using many trials with rather fine-grained measurement steps in order to determine a rather precise sensitivity estimate.

179

180

181

Apparatus and Stimuli. The experiment was conducted in a sound-attenuated room that was dimly lit with indirect, incandescent lighting. Stimuli were generated with an IBM-PC compatible computer using Matlab routines and Psychophysics Toolbox

182 extensions (Brainard, 1997; Pelli, 1997), and were presented in light gray (1.83 cd/m^2)
183 against a black (0.02 cd/m^2) background at the center of a 17-inch monitor screen
184 (1024×768 pixels screen resolution, 85-Hz refresh rate). There were four types of
185 experimental stimuli (see Figure 1): (1) a Kanizsa-type diamond shape (Kanizsa), (2)
186 a shape configuration that depicted partial contour and surface completions (Shape),
187 (3) a configuration that only induced an illusory contour without an associated surface
188 (Contour), and (4) a control configuration that consisted of four outward-facing
189 ‘pacman’ inducers, revealing a symmetric arrangement but without any emerging
190 shape (Baseline). Each pacman inducer subtended a visual angle of 1.1° . The radius of
191 the illusory diamond shape in the Kanizsa figure configuration was 3.7° of visual
192 angle. The ‘support ratio’ (Banton & Levi, 1992), that is, the ratio between the
193 luminance-defined portion and the completed illusory contour, was 0.4.

194 *Figure 1 about here*

195 **Procedure.** Observers performed a dot-localization task. Each trial started with the
196 presentation of a central fixation cross for 250 ms, followed by a 750-ms pre-cue
197 display that presented four disks in a diamond arrangement around the central fixation
198 cross. Next, one of the four configuration conditions (Kanizsa, Shape, Contour or
199 Baseline) was briefly presented for 150 ms, after which a (target) dot probe (with a
200 diameter of 8.3 arc-min) was added to the display and presented for another 100 ms
201 near the bottom left or right illusory edge of a given pacman configuration. The dot
202 probe appeared randomly at one of ten equidistant locations within a range of -53 to
203 53 arc-min along the midline perpendicular to the bottom left or right border of the
204 illusory figure (see Figure 2A for possible dot locations). Observers indicated whether
205 the dot probe was located inside or outside of the region enclosed by the inducers, by
206 pressing the left or the right button on a computer mouse, respectively. To ensure that
207 observers correctly performed the task, detailed instructions were provided
208 (<https://osf.io/3ydju/>), which also included illustrations of the correct boundary that
209 determines the inner region of the configuration (see green lines in Figure 1, bottom
210 panels). Note that the boundary of a given configuration was always located at the
211 very same position on the screen for all types of configuration. On a given trial,

212 observers were instructed to fixate the central fixation cross. The relatively short
213 duration of the dot probe (100 ms) ensured that observers could not make eye
214 movements towards it. An example trial sequence is shown in Figure 2B.

215 *Figure 2 about here*

216 Every participant completed 8 blocks of 100 trials each, resulting in 800 trials in
217 total. Every block presented one of the four configurations (Kanizsa, Shape, Contour,
218 and Baseline) with the dot appearing either in the lower left or the lower right
219 quadrant of the stimulus in separate blocks, with randomized block order across
220 participants. Note that we probed the lower left and right quadrants of the display
221 because the lower hemifield has been shown to produce a stronger percept of illusory
222 figures than the upper hemifield (Rubin, Nakayama, & Shapley, 1996). In each block,
223 a given configuration was presented with ten possible dot locations in a given
224 quadrant across ten repetitions. For the analysis, the data from the left and right
225 dot-presentation quadrants were collapsed. Before the experiment, every participant
226 was acquainted with the task in a block of 16 practice trials.

227 The fraction of ‘out’ responses was plotted against the relative dot position.
228 These data were fitted with a psychometric function $0.5 \times [1 + \gamma \times \tanh(0.745(x-\beta)/\alpha)]$,
229 where α is the discrimination threshold defined as stimulus increment from β (the
230 Point of Subjective Equivalence, PSE) to reach 82% performance (see Stanley &
231 Rubin 2003), and γ reflects the performance range. Note that the discrimination
232 threshold α is inversely related to the slope of the psychometric function (the slope at
233 the PSE is $0.3725/\alpha$) and thus gives an indication of the precision, while the PSE β
234 defines the accuracy.

235 **Results**

236 The results of Experiment 1 are depicted in Figure 3A. The psychometric curves
237 show the across-observer average fraction of ‘out’ responses as a function of dot
238 position (upper panel). The numbers on the x-axis denote the relative distances from
239 the objective boundary of the configuration, with positive values corresponding to
240 “outside” dot locations and negative values to “inside” locations (see Figure 3A; a
241 value of zero would correspond to the location of the boundary). The corresponding

242 slopes of the curves provide an estimate of the sharpness of the perceived illusory
243 figure. We defined the discrimination threshold as the dot displacement needed to
244 shift responses from 50% to 82% ‘out’ (see Methods above). The lower panel in
245 Figure 3A displays the corresponding mean discrimination thresholds (α) across
246 observers in the four conditions. To determine whether there were differences in the
247 discrimination threshold of the psychometric functions across configurations, we
248 performed a repeated-measures ANOVA with the factor configuration (Kanizsa,
249 Shape, Contour, Baseline). We additionally report the estimated Bayes factors (BF_{10})
250 as revealed by comparable Bayesian statistics using JASP (Love et al., 2015). The
251 Bayes factor provides the ratio with which the alternative hypothesis is favored over
252 the null hypothesis (i.e., larger BFs argue in favor of the alternative hypothesis with
253 values below 1 supporting the null hypothesis while values above 3 would indicate
254 moderate -, and values above 10 strong evidence in favor of the alternative hypothesis;
255 see Jeffreys, 1961; Kass & Raftery, 1995).

256 This analysis yielded a significant main effect, $F(3, 33) = 44.92, p < .0001, \eta_p^2$
257 $= .80$, 90% confidence interval, or CI [.67, .85], $BF_{10} = 6.25e+11$. For the post-hoc
258 comparisons, given that such repeated testing increases the chance of obtaining a
259 significant effect, a Bonferroni correction was applied (Neter & Wasserman, 1974).
260 Thresholds were lower in the Kanizsa condition ($M = 4.53$) compared to all other
261 conditions (Shape vs. Kanizsa: $t(11) = 3.91, p = .015, d_z = 1.13$, 95% CI [.38, 1.84],
262 $BF_{10} = 18.83$; Contour vs. Kanizsa: $t(11) = 6.45, p < .0001, d_z = 1.86$, 95% CI [.89,
263 2.80], $BF_{10} = 553.01$; Baseline vs. Kanizsa: $t(11) = 7.99, p < .0001, d_z = 2.31$, 95% CI
264 [1.19, 3.40], $BF_{10} = 3109.71$). The Shape threshold ($M = 6.17$) was lower than the
265 Contour and Baseline thresholds (Contour vs. Shape: $t(11) = 6.01, p = .001, d_z = 1.73$,
266 95% CI [.81, 2.63], $BF_{10} = 320.32$; Baseline vs. Shape: $t(11) = 7.31, p < .0001, d_z =$
267 2.11 , 95% CI [1.06, 3.13], $BF_{10} = 1489.78$). Finally, the threshold for the Contour ($M =$
268 9.95) was lower than that for the Baseline ($M = 14.56$; $t(11) = -4.32, p = .007, d_z =$
269 -1.25 , 95% CI [-2.00, -.47], $BF_{10} = 33.86$).

270 According to Figure 3A (upper panel), the Point of Subjective Equivalence (PSE,
271 50%) appeared to be shifted leftwards from the objective contour location (‘0’), in

272 particular for the Kanizsa condition. We therefore determined the PSE from the
273 psychometric function (β). The deviation from the objective contour location was
274 tested with a series of one-sample t-tests (2-tailed). Among the four configurations,
275 only the Kanizsa figure showed a significant deviation from objective contour
276 location ($M = -3.13$), $t(11) = -3.10$, $p = .01$, $d_z = -.90$, 95% CI [-1.56, -.21], $BF_{10} = 5.88$
277 (all other conditions, $ts(11) < .74$, $ps > .48$, all $d_z < .21$, all $BF_{10} < 0.36$). A potential
278 interpretation of this deviation for the Kanizsa diamond might be that observers
279 perceive the illusory contour as being curved towards the inside. Note that a
280 comparable result was also obtained in Experiments 3–5 for the Kanizsa condition
281 [$ts(11) < -3.01$, $ps < .01$, all $d_z < -.87$, all $BF_{10} > 5.15$].

282 *Figure 3 about here*

283 **Discussion**

284 The discrimination threshold of the psychometric function as derived from the
285 dot-localization performance provides an estimate of the perceptual sensitivity, that is,
286 the ‘sharpness’ of the perceived illusory figure. Experiment 1 characterized the effect
287 of surface and contour information on the discrimination thresholds as determined
288 from the psychometric functions. Our results suggest overall a high precision in
289 measuring the perceptual sensitivity with the current procedure (all $\eta_p^2 > .14$, $|d| > .8$;
290 $BF_{10} > 10$; see Cohen, 1988; Jeffreys, 1961). The threshold derived from these
291 measurements revealed to be lowest for Kanizsa figures, followed by Shape and
292 Contour configurations, indicating that the perceptual sensitivity is modulated by the
293 amount of surface information present in the configuration, with higher sensitivity –
294 as indicated by a decreased threshold and a steeper slope in the psychometric function
295 – with more surface information. In addition, we also observed that contour
296 information impacts the perception of the illusory shape, with a significantly
297 decreased threshold for Contour as compared to Baseline configurations, illustrating
298 that contours on their own can support efficient dot localization (see also Conci et al.,
299 2009). This indicates that both surface and contour completions strengthen the
300 perception of the illusory figure.

301 An additional analysis showed that the Kanizsa figure exhibited a significant

302 deviation from the objective contour location (when assuming that the illusory
303 contour renders a straight, linear boundary). This result is consistent with the view
304 that the illusory contour is actually perceived as being somewhat curved towards the
305 inside. Using Kanizsa triangles as test stimuli, Gintner, Aparajeya, Leymarie, and
306 Kovács (2016) recently observed a comparable pattern of contour curvature towards
307 the inside – a pattern in line with the current finding, indicating that the visual system
308 ultimately represents illusory contours with less precision and accuracy than
309 comparable luminance-defined contours (see also Guttman & Kellman, 2004). While
310 the contours of the Kanizsa diamond were thus perceived as slightly curved, the same
311 analysis of the PSE for the Baseline (and Shape as well as Contour conditions)
312 revealed no reliable deviation from the objective contour location. This shows that
313 participants did follow the instructions and responded based on the boundary at the
314 same location in all configurations (i.e., as illustrated by the green lines in Figure 1).

315

316

Experiment 2

317 Experiment 1 revealed a graded reduction of the discrimination threshold from
318 Baseline through Contour and Shape configurations to the Kanizsa diamond. A
319 potential explanation of this pattern might be that the computation of both the illusory
320 contours and the surface contributed to the change in precision. Alternatively, it might
321 be the contour alone which leads to a performance difference, with stronger contour
322 perception in the Kanizsa and Shape configurations compared to the Contour
323 condition (i.e., with the object's surface enhancing the strength of the contour and
324 thereby facilitating performance). To decide between these alternatives, Experiments
325 2 and 3 were performed to determine whether dot detection performance would also
326 be modulated by other forms of completion that provide a comparable amount of
327 surface filling-in, but without giving rise to a corresponding (illusory) contour.

328 For instance, besides modal completion, which was tested in Experiment 1,
329 another, related grouping phenomenon is referred to as 'amodal completion', which
330 occurs when an interpolated figure is perceived as lying behind an occluding object
331 (see Figure 4A; Michotte, Thines, & Crabbe, 1964/1991; Kanizsa, 1979; see also

332 Chen, Müller & Conci, 2016; Chen, Töllner, Müller, & Conci, 2017). Figure 1
333 provides a typical example of modal completion: a Kanizsa diamond that induces a
334 bright surface with illusory contours. In comparison, in the example depicted in
335 Figure 4A, an integrated diamond is perceived as well, but it appears to be completed
336 behind the four circular apertures. Thus, in this case, the diamond shape is completed
337 behind the occluding region, and as a result, the illusory contour is not directly visible
338 (see illustration in Figure 4A, and Michotte et al., 1964/1991). Thus, in the
339 configurations in Figure 4B, surface completion remains to connect disparate parts of
340 the figures (e.g., in the Kanizsa and Shape conditions), but there is no crisp boundary
341 forming an illusory contour (e.g. in all configurations presented in Figure 4B).

342 Experiment 2 used a similar paradigm to that described for Experiment 1 and
343 investigated how the dot-localization sensitivity is affected by amodal completion (as
344 opposed to modal completion in Experiment 1), that is, when the illusory contours are
345 not visible due to partial occlusion. If surface processing contributes to our
346 performance measure and is dissociable from the completion of (illusory) contours,
347 then perceptual sensitivity would be expected to be modulated by surfaces even when
348 no precise bounding contour is available.

349 **Method**

350 Experiment 2 was basically identical to Experiment 1, with the following
351 differences: 12 right-handed paid volunteers (7 men; mean age: 23.5 ± 2.15 years;
352 normal or corrected-to-normal vision) participated in the experiment. Stimuli in
353 Experiment 2 were designed to induce amodal completion. The stimulus
354 arrangements were identical to those revealing modal completion in Experiment 1,
355 except that a gray outline circle was added to surround each pacman inducer (line
356 thickness: 9 arc-min; see Figure 4B).

357 *Figure 4 about here*

358 **Results**

359 The upper panel in Figure 3B displays the psychometric curves (averaged across
360 observers) as a function of dot position, separately for the different configuration
361 conditions. In addition, the lower panel of Figure 3B shows the corresponding mean

362 discrimination thresholds. A repeated-measures ANOVA with the factor configuration
363 (Kanizsa, Shape, Contour, Baseline)¹ again revealed a significant effect, $F(3, 33) =$
364 $20.76, p < .0001, \eta_p^2 = .65, 90\% \text{ CI } [.44, .73], BF_{10} = 9.43e+4$. The thresholds were
365 lower for Kanizsa ($M = 12.63$) and Shape ($M = 13.62$) than for Contour ($M = 19.44$)
366 and Baseline ($M = 18.55$) configurations (Contour vs. Kanizsa: $t(11) = 6.53, p < .0001,$
367 $d_z = 1.88, 95\% \text{ CI } [.91, 2.83], BF_{10} = 603.42$; Baseline vs. Kanizsa: $t(11) = 4.44, p$
368 $= .006, d_z = 1.28, 95\% \text{ CI } [.49, 2.04], BF_{10} = 40.29$; Contour vs. Shape: $t(11) = 9.01, p$
369 $< .0001, d_z = 2.60, 95\% \text{ CI } [1.38, 3.80], BF_{10} = 8.64e+3$; Baseline vs. Shape: $t(11) =$
370 $4.33, p = .007, d_z = 1.25, 95\% \text{ CI } [.47, 2.00], BF_{10} = 34.27$). There were no significant
371 threshold differences between Kanizsa and Shape, $t(11) = .87, p > .99, d_z = .25, 95\%$
372 $\text{ CI } [-.33, .82], BF_{10} = 0.40$, or between Contour and Baseline configurations, $t(11)$
373 $= .92, p > .99, d_z = .27, 95\% \text{ CI } [-.32, .84], BF_{10} = 0.41$.

374 A further analysis then compared all configurations across Experiments 1 and 2.
375 To this end, we performed a mixed-design ANOVA with the within-subjects factor
376 configuration and the between-subjects factor experiment. This analysis revealed a
377 main effect of configuration, $F(3, 66) = 57.28, p < .0001, \eta_p^2 = .72, 90\% \text{ CI } [.61, .77],$
378 $BF_{10} = 5.03e+13$, with lower thresholds for Kanizsa and Shape than for either Contour
379 or Baseline configurations, $ts(11) > 7.66, ps < .0001$, all $d_z > 1.56$, all $BF_{10} > 1.66e+5$;
380 and a main effect of experiment, $F(1, 22) = 18.32, p < .0001, \eta_p^2 = .45, 90\% \text{ CI}$
381 $[.18, .62], BF_{10} = 86.52$, with higher thresholds in Experiment 2 ($M = 16.06$) than in
382 Experiment 1 ($M = 8.80$). The interaction between configuration and experiment was
383 also significant, $F(3, 66) = 5.43, p = .002, \eta_p^2 = .20, 90\% \text{ CI } [.05, .31], BF_{10} = 14.45$:
384 there was no significant difference in thresholds between experiments for Baseline
385 configurations, $t(11) = 1.91, p = .07, d = .78, 95\% \text{ CI } [-.06, 1.61], BF_{10} = 1.34$, but
386 thresholds were overall higher in Experiment 2 than in Experiment 1 for Kanizsa,
387 Shape, and Contour configurations, $ts(11) > 3.73, ps < .001$, all $d > 1.52$, all $BF_{10} >$
388 26.95 .

¹ It should be noted that a Kanizsa figure is typically an example of modal completion – so that the term “Kanizsa”, in a strict sense, would only be appropriate when describing the diamond stimulus as used in Experiment 1. However, for the sake of consistency (i.e., for providing a coherent terminology when describing our experimental manipulations), we nevertheless used comparable labels for our conditions throughout all experiments in this study.

389 **Discussion**

390 Experiment 2 presented amodal completion stimuli, where the illusory figure is
391 perceived as being partially occluded. The results of Experiment 2 suggest that
392 surface completion influences performance despite the occlusion, as amodal variants
393 of Kanizsa and Shape configurations still exhibited a higher dot-localization
394 sensitivity than corresponding Contour and Baseline stimuli. It should be noted in this
395 regard that there was no significant difference in sensitivity when comparing the
396 amodally completed contour and baseline configurations (the threshold for Contour
397 was numerically even higher than for Baseline). This confirms that an illusory contour
398 is not effectively completed across an occluder, but nevertheless an occluded region
399 still modulates detection performance.

400 The occluded configurations in Experiment 2 led to an overall decreased
401 sensitivity of dot localization for stimuli that induce an illusory region (Kanizsa,
402 Shape, and Contour configurations), as compared to Experiment 1 with comparable
403 modal-completion stimuli. However, no significant difference between the two
404 experiments was found in the Baseline, suggesting that the performance reduction
405 occurred because of the increased difficulty in processing the occluded object, but not
406 because of a potential difference in perceptual complexity of the configurations that
407 may have resulted from the addition of the outline circles.

408 To further substantiate that the non-significant differences between Kanizsa and
409 Shape ($d_z = .25$), and between Contour and Baseline configurations ($d_z = .27$) were
410 not due to a lack of statistical power, we conducted a second post-hoc power analysis,
411 again setting power to 80% and the alpha level to .05 (two-tailed). In Experiment 1,
412 the effect size of the smallest numerical contrast (i.e. between Kanizsa and Shape
413 conditions) was 1.13, thus, revealing a large effect (cf. Cohen, 1988). The power
414 analysis in fact showed that our current sample size would be sufficient to detect such
415 an effect size. It is therefore unlikely that our non-significant effects can be attributed
416 to a limitation in sample size. Moreover, an additional estimation of the Bayes factor
417 for these non-significant differences revealed that both the comparisons between
418 Kanizsa and Shape ($BF_{10} = 0.40$) and between Contour and Baseline ($BF_{10} = 0.41$)

419 were clearly in favor of the null hypothesis.

420

421

Experiment 3

422 Experiment 2 provided clear evidence for a surface-based modulation of
423 performance even though no illusory contour was visible in the presented (amodal)
424 configurations. It could be argued, however, that amodal completion (i.e., the
425 grouping of an object behind an occluder) is, in crucial ways, different from modal
426 completion (e.g., in “standard” Kanizsa figures as tested in Experiment 1; see Murray,
427 Foxe, Javitt, & Foxe, 2004). Experiment 3 was therefore performed to further
428 investigate whether a performance modulation for surface-defined groupings (without
429 a concurrent illusory contour) could also be demonstrated in cases of modal
430 completion. To this end, configurations were presented with smoothed pacman
431 inducers, which, in previous studies, have been shown to reveal surface completion,
432 that is, affording selection based on a “salient region” (Shipley & Kellman, 1990;
433 Stanley & Rubin, 2003), without a corresponding illusory contour (see Figure 5). If
434 dot-localization sensitivity is modulated by the presence of a salient region alone, then
435 surface filling-in and contour interpolation might be considered separate mechanisms
436 that contribute to the completion of an illusory figure in both variants of modal and
437 amodal completion.

438 *Method*

439 Experiment 3 was again basically identical to Experiments 1 and 2, with the
440 following differences: 12 right-handed paid volunteers (5 men; mean age: $25.92 \pm$
441 5.57 years; normal or corrected-to-normal vision) participated in the experiment.
442 There were two possible stimulus configurations: Kanizsa configurations, consisting
443 of a salient, central object, were compared to Baseline configurations (i.e., stimulus
444 arrangements that do not give rise to any emerging shape). In addition, these two
445 types of configuration could be presented with two types of inducers, or edges
446 (“sharp” and “smoothed”), resulting in four possible conditions: stimuli with “sharp”
447 edges were essentially identical to the configurations presented in Experiment 1 (see
448 Figure 5), whereas the sharp corners of the inducer shapes were eliminated in

449 configurations with “smoothed” edges. In the smoothed variant of the Kanizsa
450 configuration, this change of the inducers created the impression of an enclosed
451 “salient region”, but without a crisp bounding contour (Shipley & Kellman, 1990;
452 Stanley & Rubin, 2003; see Figure 5). Smoothed inducers were generated by
453 manually tracing the outlines of the inducers to eliminate their sharp corners and then
454 rotating each inducer by 10 degrees clockwise to eliminate the alignment of the
455 straight parts of the edges. This procedure was similar to previous studies, which also
456 used smoothed inducers (e.g., Stanley & Rubin, 2003).

457 *Figure 5 about here*

458 **Results**

459 Figure 6 presents the psychometric curves (top) and the corresponding mean
460 discrimination thresholds (bottom) for the different conditions in Experiment 3 (upper
461 and lower panels, respectively). A repeated-measures ANOVA with the factors
462 configuration (Kanizsa, Baseline) and edge (sharp, smoothed) on the discrimination
463 thresholds revealed a significant main effect of configuration, $F(1, 11) = 40.10, p$
464 $< .0001, \eta_p^2 = .79, 90\% \text{ CI } [.49, .86], BF_{10} = 6.59e+4$: thresholds were lower for
465 Kanizsa ($M = 8.35$) than for Baseline configurations ($M = 16.05$). The main effect of
466 edge was not significant, $F(1, 11) = 3.91, p = .07, \eta_p^2 = .26, 90\% \text{ CI } [0, .52], BF_{10}$
467 $= .54$, and there was also no interaction effect, $F(1, 11) = 1.47, p = .25, \eta_p^2 = .12, 90\%$
468 $\text{CI } [0, .39], BF_{10} = .68$. However, despite of the non-significant interaction, paired-t
469 tests still revealed a significantly lower threshold for the Kanizsa configuration with
470 sharp edges than that with smoothed edges, $t(11) = -2.74, p = .019, d_z = -.79, 95\% \text{ CI}$
471 $[-1.43, -.12], BF_{10} = 3.49$, while there was no difference between the two edge types
472 for Baseline configurations, $t(11) = -.30, p = .77, d_z = -.09, 95\% \text{ CI } [-.65, .48], BF_{10}$
473 $= .30$.

474 *Figure 6 about here*

475 **Discussion**

476 Experiment 3 compared performance for Kanizsa and Baseline configurations
477 with sharp and smoothed edges. In the Kanizsa configuration with smoothed edges,
478 surface completion mechanisms typically render the impression of a closed, “salient

479 region” that is perceived (even) without concurrent illusory contours (Stanley &
480 Rubin, 2003). Accordingly, the results of Experiment 3 suggest that salient-region
481 computations influence dot-localization performance even in the absence of illusory
482 contours – as evidenced by a consistently higher sensitivity for Kanizsa as compared
483 to Baseline configurations, independently of the type of edge (sharp or smoothed).
484 Although the interaction was non-significant, there was still a significant difference
485 between Kanizsa configurations with sharp and smoothed edges, consistent with
486 Stanley and Rubin (2003) who used comparable stimuli and the same task. This
487 pattern suggests that both surface information and contour processing contributed to
488 the observed modulation of dot-localization sensitivity. For the Baseline condition, by
489 contrast, there was no difference between configurations with smoothed and sharp
490 edges, that is, the subtle physical difference between the two types of inducers alone
491 did not impact the basic level of performance.

492 Together, Experiments 2 and 3 show that surface filling-in can facilitate the
493 perception of modally and amodally completed configurations, over and above any
494 contribution from the interpolation of illusory contours (e.g., as revealed in
495 Experiment 1). This indicates that illusory contours and salient surfaces are computed
496 by separate mechanisms that do not necessarily depend on each other.

497

498

Experiment 4

499 Across Experiments 1 to 3, an increased sensitivity was revealed for the Kanizsa
500 figure as compared to configurations that do not induce a comparable illusory shape
501 (e.g., the Baseline configuration). As outlined above, this difference can be explained
502 by grouping mechanisms, according to which localization of the dot is more accurate
503 when an illusory shape allows estimation of the precise position of the target dot in
504 relation to the illusory figure. However, a potential alternative account may simply be
505 that the advantage for the Kanizsa figure results from the shorter spatial distance
506 between the edges of the two inward-facing pacmen in the Kanizsa figure, as
507 compared to a somewhat larger distance between edges in the two outward-facing
508 pacmen in the Baseline condition (see Figure 7A, left and middle panels for an

509 illustration). Note that this latter account would attribute the observed differences in
510 performance primarily to the distance between the edges of a configuration, rather
511 than to the completion of an illusory figure. To exclude this potential confound, in
512 Experiment 4, we equated the distances between the edges of two neighboring
513 pacmen using rectangular variants of the Kanizsa figure and the Baseline
514 configuration of Experiment 1.

515 **Method**

516 Experiment 4 was largely identical to Experiment 1, with the following
517 differences: 12 right-handed paid volunteers (7 men; mean age: 25 ± 3.10 years;
518 normal or corrected-to-normal vision) participated in the experiment. There were
519 again four possible stimulus configurations in the experiment: The ‘Smaller’ Kanizsa
520 and Baseline configurations were identical to the ones presented previously in
521 Experiment 1. Two additional configurations presented larger, rectangular stimulus
522 arrangements (the “Larger Kanizsa” and “Larger Baseline” configurations). For the
523 larger Kanizsa configuration, the distance between the edges of the two pacmen on
524 the side where the target dot appeared was the same as that of the original Baseline
525 configuration in Experiment 1 (see Figure 7A, right and middle panels, respectively).
526 The support ratio for the larger Kanizsa diamond was 0.29. The larger Baseline
527 configuration was identical to the Baseline condition (also presenting no illusory
528 object), but with the pacman inducers placed at same distances as for the larger
529 Kanizsa stimulus configuration. These additional larger variants of the configurations
530 permitted assessment of the effect of contour length on performance, while keeping
531 the distance between the central fixation cross and the dot constant (for examples of
532 the actual stimuli, see Figure 7B).

533 *Figure 7 about here*

534 **Results**

535 Figure 8 presents the psychometric curves for the different conditions and the
536 corresponding mean discrimination thresholds in Experiment 4 (upper and lower
537 panels, respectively). A repeated-measures ANOVA with the factors configuration
538 (Kanizsa, Baseline) and size (smaller, larger) on the discrimination thresholds

539 revealed a significant main effect of configuration, $F(1, 11) = 73.54, p < .0001, \eta_p^2$
540 $= .87, 90\% \text{ CI } [.65, .92], BF_{10} = 1.16e+7$, with lower thresholds for Kanizsa ($M = 9.07$)
541 than for Baseline configurations ($M = 20.08$). In addition, the main effect of size was
542 significant, $F(1, 11) = 5.77, p = .035, \eta_p^2 = .34, 90\% \text{ CI } [.01, .58], BF_{10} = 0.54$:
543 thresholds were lower for the smaller ($M = 13.20$) than for larger configurations ($M =$
544 15.95) – though with the BF_{10} value providing no conclusive support for the
545 alternative hypothesis. There was no interaction effect, $F(1, 11) = .18, p = .68, \eta_p^2$
546 $= .02, 90\% \text{ CI } [0, .23], BF_{10} = 0.37$. Theoretically of most importance, when equating
547 the spatial distance between the edges of a configuration, there was still a significant
548 difference between the smaller Baseline and the larger Kanizsa configuration, $t(11) =$
549 $4.78, p = .001, d_z = 1.38, 95\% \text{ CI } [.56, 2.17], BF_{10} = 64.75$: the threshold was lower
550 for the larger Kanizsa ($M = 10.75$) than for the smaller Baseline configuration ($M =$
551 19.01).

552 *Figure 8 about here*

553 **Discussion**

554 Experiment 4 replicated the results of Experiment 1, in revealing a lower
555 threshold for the larger Kanizsa configuration than for the Baseline even when
556 controlling for the distance between the pacman inducers on the side on which the
557 target dot appeared. This result indicates that the decreased discrimination threshold
558 for the Kanizsa figure in Experiments 1 to 3 was not caused by variations in spatial
559 distance between neighboring inducers in the various configurations. Rather,
560 dot-localization sensitivity appears to be distinctly influenced by the completion of an
561 illusory figure.

562 Moreover, Experiment 4 showed that sensitivity is reduced for the larger as
563 compared to the smaller configurations, with this difference in size showing a
564 particularly strong variation for the comparison between large and small Kanizsa
565 figures ($t(11) = 4.94, p < .0001, d_z = 1.43, 95\% \text{ CI } [.59, 2.23], BF_{10} = 80.45$). This
566 result suggests that the support ratio (i.e., the relation between the inducer disks and
567 the illusory contour) determines the strength of the illusory figure and, as a result,
568 perceptual sensitivity. This outcome is consistent with previous findings, which

569 suggest that, although perceptual interpolation of subjective contours appears to be
570 instantaneous and effortless, interpolation is constrained by spatial factors such as
571 inducer size, inducer spacing, and overall size of the display. Larger inducers and
572 smaller spacing between inducers have previously been shown to increase the
573 subjective clarity of the interpolated contours (Watanabe & Oyama, 1988; Shipley &
574 Kellman, 1992), suggesting that the perception of illusory contours is strongly tied to
575 the support ratio (e.g., Banton & Levi, 1992; Kojo, Liinasuo, & Rovamo, 1993).

576

577

Experiment 5

578 Experiment 4 ruled out the possibility that the advantage for the Kanizsa figure is
579 due to the shorter spatial distances between the edges of the pacman inducers.
580 However, an alternative explanation for our findings could be that the decreased
581 sensitivity in the Baseline (relative to the Kanizsa) configuration is owing to the edge
582 interruption by the inducer surface, which increases the difficulty of computing a
583 boundary. That is, the pacman inducer with outward-oriented indent would impede the
584 formation of a connecting line between the inducer edges in the Baseline, but not in
585 the Kanizsa configuration, thus impeding the accuracy with which the inside-outside
586 judgment can be made. To exclude this potential confound, in Experiment 5, we
587 eliminated the visual interruption by using variants of inducer elements that simply
588 consisted of collinearly arranged L-shaped line junctions (see examples in Figure 9).
589 In addition, we controlled for spatial distance between the edges of the inducers in the
590 different configurations (comparable to the procedure adopted in Experiment 4).
591 Processing of object configurations is usually found to be equally efficient for shapes
592 composed of circular inducers and line segments (e.g., in visual search; see Conci et
593 al., 2007a; 2007b). We therefore expected that dot-localization performance would be
594 modulated by the closure of the presented configurations (i.e., revealing a benefit for
595 the Kanizsa configurations relative to the Baseline) regardless of the presence or
596 absence of a visual interruption caused by the inducers (pacmen vs. line junctions).

597 *Method*

598 Experiment 5 was comparable to Experiment 4, with the following differences: 12

599 right-handed paid volunteers (6 men; mean age: 24.25 ± 2.56 years; normal or
600 corrected-to-normal vision) participated in the experiment. There were again four
601 possible stimulus configurations: First, the Kanizsa and Baseline configurations were
602 presented with pacman inducers, similar to those in Experiment 4. Second, two
603 additional configurations were presented that consisted of four L-shaped corner
604 junctions, with the length of each line (1.1° ; line thickness: 6 arc-min) being identical
605 to the radius of the pacman inducers (see example stimuli with line inducers in Figure
606 9). The corner junctions were arranged in a diamond-like form, and either presented a
607 closed shape (Kanizsa) or a corresponding open, cross-shaped (Baseline)
608 configuration. The pacman and line inducers in the Baseline configurations were
609 placed at the same distance as in the Kanizsa configurations (on the side where the dot
610 probe appeared, see Figure 9) – resulting in rectangular baseline arrangements, which
611 allowed performance to be assessed across the various configurations independently
612 of variations of the task-critical boundary (see above, Experiment 4). All other details
613 of the Kanizsa and Baseline configurations with line inducers were identical to the
614 corresponding configurations with pacman inducers.

615 *Figure 9 about here*

616 **Results**

617 The psychometric curves and the corresponding mean discrimination thresholds
618 for the different conditions are presented in Figure 10 (upper and lower panels,
619 respectively). A repeated-measures ANOVA with the factors configuration (Kanizsa,
620 Baseline) and inducer type (pacman, line) on the discrimination thresholds revealed a
621 significant main effect of configuration, $F(1, 11) = 37.11, p < .0001, \eta_p^2 = .77, 90\% \text{ CI}$
622 $[.46, .85], BF_{10} = 4.28e+4$, again with lower thresholds for Kanizsa ($M = 6.24$) than
623 for Baseline configurations ($M = 12.11$). In addition, the configuration \times inducer type
624 interaction was significant, $F(1, 11) = 10.58, p = .008, \eta_p^2 = .49, 90\% \text{ CI} [.1, .67],$
625 $BF_{10} = 6.12$, due to there being a significant difference between the pacman and line
626 inducers for the Baseline configuration, $t(11) = 2.49, p = .03, d_z = .72, 95\% \text{ CI} [.07,$
627 $1.35], BF_{10} = 2.47$, but no significant difference for the Kanizsa configuration, $t(11) =$
628 $1.59, p = .14, d_z = .46, 95\% \text{ CI} [-.15, 1.05], BF_{10} = .77$. Note, though, that a significant

629 reduction of the threshold for Kanizsa relative to Baseline configurations was found
630 for both types of inducer: pacman inducers: $t(11) = 6.42, p < .0001, d_z = 1.85, 95\% \text{ CI}$
631 $[.89, 2.79], BF_{10} = 530.97$; and line inducers: $t(11) = 2.95, p = .01, d_z = .85, 95\% \text{ CI}$
632 $[.17, 1.51], BF_{10} = 4.75$. Finally, there was no effect of inducer type, $F(1, 11) = .62,$
633 $p = .45, \eta_p^2 = .05, 90\% \text{ CI} [.00, .30], BF_{10} = .33$.

634 As can be seen from Figure 10 (upper panel), the PSE appears to be shifted from
635 the objective contour location, in particular for the Kanizsa configurations. We
636 therefore tested the deviation from the objective location with a series of one-sample
637 t-tests (2-tailed), as in Experiment 1. Both the PSE of the Kanizsa configurations with
638 pacman and line inducers showed a significant deviation from the objective contour
639 location, but interestingly in opposite directions: as in Experiment 1, the pacman
640 version of the Kanizsa configuration exhibited a deviation towards inside locations (M
641 $= -3.74$), $t(11) = -3.01, p = .012, d_z = -.87, 95\% \text{ CI} [-1.52, -.19], BF_{10} = 5.15$; by
642 contrast, the line-inducer version of the Kanizsa configuration showed a deviation
643 towards outside locations ($M = 5.43$), $t(11) = 2.38, p = .036, d_z = .69, 95\% \text{ CI} [.04,$
644 $1.31], BF_{10} = 2.12$. [All Baseline conditions, $ts(11) < 1.9, ps > .08$, all $d_z < .55$, all
645 $BF_{10} < 1.1$.]

646 *Figure 10 about here*

647

648 **Discussion**

649 Experiment 5 revealed a reduced dot-localization sensitivity for Baseline than for
650 Kanizsa configurations, which was largely independent of inducer type. This shows
651 that the observed performance difference can be attributed to the completion of an
652 illusory figure, which enhances perceptual sensitivity irrespective of any visual edge
653 interruption produced by the pacman inducer surface (in the Baseline condition).
654 However, despite a clear effect of grouping upon performance, the interruption
655 nevertheless modulated the efficiency of dot localization in the Baseline
656 configurations. In particular, thresholds were reduced in Baseline configurations with
657 (non-interrupted) line inducers as compared to (interrupted) pacman inducers
658 –showing that without an emergent figure, the computation of a task-relevant object

659 boundary depends on the efficiency with which inducers can be integrated to form a
660 connecting line. Of note, this finding is essentially the same as the reduction of
661 sensitivity in Experiment 2 relative to Experiment 1, where the addition of circular
662 rings to the inducers (in Experiment 2) resulted in an overall performance decrease
663 due to the interruption of the connection between neighboring pacman inducers.

664 In addition, Experiment 5 revealed another interesting result, namely: the PSE
665 for Kanizsa configurations with pacman and line-inducers deviated from the objective
666 contour location in opposing directions. In particular, participants tended to perceive
667 the boundary of the Kanizsa configuration with pacman inducers as being curved
668 towards the inside (as in Experiment 1), and with line inducers as being curved
669 towards the outside. Comparable findings were reported in previous studies with
670 pacman (Guttman & Kellman, 2004; Gintner et al., 2016) and line (Gegenfurtner,
671 Brown, & Rieger, 1997; Conci et al., 2007b) inducers. With the line inducers, this
672 ‘outside’ bias might arise because observers perceive an illusory square that appears
673 to be completed in front of the L-inducer, diamond-shaped grouping.

674

675 **General Discussion**

676 In the current study, we probed the sensitivity of illusory figure perception by
677 means of a dot-localization task, and established separable influences of contour- and
678 surface-related processing by gradually manipulating various aspects of grouping in
679 the stimulus configurations. Sensitivity was estimated from the discrimination
680 threshold of the psychometric functions of dot-localization performance: the lower the
681 discrimination threshold (i.e., the steeper the slope), the higher the sensitivity.
682 Experiment 1 showed that sensitivity was modulated by both the amount of surface
683 and contour information present in a given configuration, with the highest sensitivity
684 for (complete) Kanizsa figures, followed by Shape and Contour configurations, and
685 the lowest sensitivity for the Baseline configuration. This pattern indicates that both
686 surface filling-in and contour interpolation contribute to the formation of the illusory
687 figure. In Experiment 2, the same experimental logic was applied to occluded object
688 configurations. For the amodally completed stimuli, the sensitivity was overall

689 reduced (i.e., in Kanizsa, Shape, and Contour stimuli). In addition, while the
690 difference between Contour and Baseline stimuli disappeared, Kanizsa and Shape
691 configurations still afforded higher sensitivity than Contour and Baseline
692 configurations – suggesting that the formation of an illusory surface continued to
693 facilitate performance even when contour interpolation processes were not available
694 (due to object occlusion). Next, in Experiment 3, separable processing of contour and
695 surface information was further investigated by presenting modal completion
696 configurations with smoothed inducers, which group to form a coherent surface
697 region but without concurrent illusory contours. The results from these
698 “salient-region” stimuli again showed an increased perceptual sensitivity relative to
699 the Baseline configurations. Thus, together, the results of Experiments 2 and 3
700 consistently show that contour and surface processing can be dissociated to some
701 extent in the completion of an illusory figure, that is, they provide separable
702 influences on performance. Finally, Experiments 4 and 5 were performed as control
703 experiments to confirm that the performance benefit for Kanizsa figures was due to
704 the completion of an illusory figure, rather than being attributable to subtle variations
705 in distance between the pacman elements in the configurations presented (Experiment
706 4), or due to visual (edge) interruption which interferes with the computation of a
707 boundary in the Baseline configuration (Experiment 5).

708 Taken together, our results support the view that the completion of illusory
709 contours and surfaces provide essential contributions to the formation of illusory
710 Kanizsa figures, as both contribute to dot-localization performance (see Experiments
711 1–3). This supports common explanations of the underlying mechanisms of modal
712 completion (see Pessoa et al., 1998, for a review), and is consistent with previous
713 observations that both processes of surface and contour grouping are available
714 preattentively (Conci et al., 2009; see also Mattingley, Davis, & Driver, 1997). At the
715 same time, however, the results are, to some extent, inconsistent with findings from
716 visual search, which indicated that only the surface but not the surrounding contours
717 determine the efficiency of detecting Kanizsa figure targets among distractors (Conci
718 et al., 2007a). This difference in results is likely attributable to differential task

719 requirements, as the role of contour interpolation might be underestimated in a visual
720 search task where attention is to be focused on a relatively broad representation of the
721 Kanizsa target shape (see also Stanley & Rubin, 2003). In this view, the allocation of
722 attention appears to be determined by the specifics of a given task: a relatively broad
723 estimation of a salient region might suffice to detect an illusory square in visual
724 search, whereas the dot-localization task engenders more precise discrimination
725 processes that require the engagement of both contour and surface completion to
726 render a more precise shape representation.

727 In general, mechanisms of figure-ground segregation are thought to be involved
728 in integrating inducer information so as to represent an illusory surface as lying in
729 front of the pacman inducer disks (Kogo et al., 2010; Kogo & Wagemans, 2013). Note
730 that we found that surface construction processes yield a performance benefit even
731 when illusory contours are not perceived due to occlusion (Experiment 2), or as a
732 result of smoothed pacmen inducers (Experiment 3). Although it is not possible to
733 perceive explicit, definitive contours with these variants of the illusory objects,
734 observers nevertheless appeared to perceive the continuation of the surface behind the
735 pacmen, or a salient region that was formed in the absence of sharp boundaries, and,
736 as a result, detected the illusory shape, leading to an increase of their perceptual
737 sensitivity (see also Van Lier, 1999).

738 To explain how Kanizsa figures are completed, it has been proposed that
739 processing of the illusory figure is accomplished by a feedforward, serial mechanism
740 (Grosopf, Shapley, & Hawken, 1993; Ffytche & Zeki, 1996), during the operation of
741 which surface filling-in is achieved only after the interpolation of the respective
742 illusory contours. In this view, the boundaries of an object are computed first and the
743 surface is generated only afterwards. However, the present results provide strong
744 evidence that illusory contours and the corresponding surfaces are computed by
745 separate mechanisms that are not necessarily dependent on each other (see also
746 Grossberg & Mingolla, 1985; Drespf & Bonnet, 1991; Drespf, Lorenceau, & Bonnet,
747 1990; Rogers-Ramachandran & Ramachandran, 1998). In fact, illusory surfaces can
748 be generated without an exact specification of the illusory contours that demarcate the

749 object boundaries (Experiments 2 and 3; see also Stanley & Rubin, 2003). This
750 pattern, of separable processing of contours and surfaces, is difficult to explain by a
751 serial, feedforward process. Arguably, a better explanation is provided by recurrent
752 models of completion, on which completion of illusory figures results from a series of
753 feedforward and feedback loops, with processing operating in parallel at various
754 levels in the visual hierarchy (Lamme & Roelfsema, 2000; Roelfsema, Lamme,
755 Spekreijse, & Bosch, 2002; Kogo et al., 2010; Kogo & Wagemans, 2013). On such a
756 recurrent-network account, different object components may be specified with relative
757 independence of each other. For instance, parallel, feedforward processing may
758 initially extract contours and surfaces independently of each other via separate
759 mechanisms. The combination of their outputs is then accomplished by a recurrent
760 feedback process that combines the estimated surface with the associated contours to
761 form a coherent whole.

762 In line with this account, Stanley and Rubin (2003) reported fMRI evidence
763 suggesting that the visual system first detects the “salient regions” of an object at
764 higher cortical levels (e.g., in the LOC; Seghier & Vuilleumier, 2006), and this crude
765 region estimation is then complemented by contour-sensitive processes in lower
766 cortical regions (V1/V2 regions) through a top-down feedback loop that, in turn,
767 refines the perception of the surface and determines its precise edges. Moreover,
768 Shpaner, Molholm, Forde, and Foxe (2013) reported evidence to suggest that the flow
769 of information via feedforward and feedback connections across various levels in the
770 visual hierarchy facilitates the perception of the whole illusory figure. In general
771 agreement with these accounts, the current findings show that completion of illusory
772 contours is supported by complementary processes of surface filling-in, yielding
773 higher sensitivity for Kanizsa and Shape compared to Contour configurations (see
774 Experiment 1). This might be the result of a refined object representation that first
775 extracts the respective surface and contour information, with subsequent, recurrent
776 feedback iterations combining these sources of information to represent the whole
777 illusory figure.

778

Conclusions

779 Object completion – as exemplified in the Kanizsa figure – is a fundamental
780 operation of human vision and observed in many instances, with the representation of
781 a coherent whole determining all subsequent higher-order cognitive and emotional
782 processing (see, e.g., Erle, Reber, & Topolinski, 2017). Thus, identification of the
783 mechanisms underlying object completion (in Kanizsa figures) is essential for a
784 complete understanding of human vision. The current study established an approach
785 for effectively investigating these mechanisms by examining illusory figure
786 sensitivity using a dot-localization task while comparing and contrasting the relative
787 impact of the available contour and surface information. Collectively, the results
788 obtained provide further support for a multi-stage model of object processing. Illusory
789 contour and surface completions are both closely related to fundamental mechanisms
790 of the visual system by which illusory figures are grouped, interacting through a series
791 of feedforward and feedback loops.

792

793 **Acknowledgments**

794 This work was supported by project grants from the German Research
795 Foundation (DFG; FOR 2293/1). Siyi Chen received a scholarship from the China
796 Scholarship Council (CSC).

797 **Open Practices**

798 All data and materials have been made publicly available via the open science
799 framework and can be accessed at <https://osf.io/3ydju/>.

800 **References**

- 801 Banton, T., & Levi, D. M. (1992). The perceived strength of illusory contours.
802 *Perception & Psychophysics*, *52*, 676–684.
- 803 Bakar, A. A., Liu, L., Conci, M., Elliott, M. A., & Ioannides, A. A. (2008). Visual field
804 and task influence illusory figure responses. *Human Brain Mapping*, *29*(11),
805 1313–1326.
- 806 Brainard, D. H. (1997). The psychophysics toolbox. *Spatial Vision*, *10*, 433-436.
- 807 Chen, S., Müller, H. J., & Conci, M. (2016). Amodal completion in visual working
808 memory. *Journal of Experimental Psychology: Human Perception and*

809 *Performance*, 42(9), 1344–1353.

810 Chen, S., Töllner, T., Müller, H. J., & Conci, M. (2017). Object maintenance beyond
811 their visible parts in working memory. *Journal of Neurophysiology*, jn-00469.

812 Cohen, J. (1988). *Statistical power analysis for the behavioral sciences*. Lawrence
813 Erlbaum Associates, Hillsdale, NJ.

814 Conci, M., Böbel, E., Matthias, E., Keller, I., Müller, H. J., & Finke, K. (2009).
815 Preattentive surface and contour grouping in Kanizsa figures: Evidence from
816 parietal extinction. *Neuropsychologia*, 47(3), 726–732.

817 Conci, M., Gramann, K., Müller, H. J., & Elliott, M. A. (2006). Electrophysiological
818 correlates of similarity-based interference during detection of visual forms.
819 *Journal of Cognitive Neuroscience*, 18(6), 880–888.

820 Conci, M., Müller, H. J., & Elliott, M. A. (2007a). The contrasting impact of global
821 and local object attributes on Kanizsa figure detection. *Attention, Perception &*
822 *psychophysics*, 69(8), 1278–1294.

823 Conci, M., Müller, H. J., & Elliott, M. A. (2007b). Closure of salient regions
824 determines search for a collinear target configuration. *Attention, Perception, &*
825 *Psychophysics*, 69(1), 32-47.

826 Cornsweet, T. N. (1970). *Visual perception*. San Diego, California: Harcourt Brace.

827 Davis, G., & Driver, J. (1994). Parallel detection of Kanizsa subjective figures in the
828 human visual system. *Nature*, 371, 291–293.

829 Dresch, B., & Bonnet, C. (1991). Psychophysical evidence for low-level processing of
830 illusory contours and surfaces in the Kanizsa square. *Vision Research*, 31,
831 1813–1817.

832 Dresch, B., Lorenceau, J., & Bonnet, C. (1990). Apparent brightness enhancement in
833 the Kanizsa square with and without illusory contour formation. *Perception*, 19,
834 483–489.

835 Erdfelder, E., Faul, F., & Buchner, A. (1996). GPOWER: A general power analysis
836 program. *Behavior research methods, instruments, & computers*, 28(1), 1-11.

837 Erle, T. M., Reber, R., & Topolinski, S. (2017). Affect from mere perception: Illusory
838 contour perception feels good. *Emotion*, 17(5), 856.

839 Ffytche, D. H., & Zeki, S. (1996). Brain activity related to the perception of illusory
840 contours. *NeuroImage*, 3, 104–108.

841 Gegenfurtner, K. R., Brown, J. E., & Rieger, J. (1997). Interpolation processes in the
842 perception of real and illusory contours. *Perception*, 26(11), 1445-1458.

843 Gintner, T., Aparajeya, P., Leymarie, F. F., & Kovács, I. (2016). Curvy is the new
844 straight: Kanizsa triangles. *Perception*, 45(S2), 44..

845 Grosz, D. H., Shapley, R. M., & Hawken, M. J. (1993). Macaque-V1 neurons can
846 signal illusory contours. *Nature*, 365, 550–552.

847 Grossberg, S., & Mingolla, E. (1985). Neural dynamics of form perception: Boundary
848 completion, illusory figures and neon color spreading. *Psychological Review*, 92,
849 173–211.

850 Guttman, S. E., & Kellman, P. J. (2004). Contour interpolation revealed by a dot
851 localization paradigm. *Vision Research*, 44(15), 1799-1815.

852 Hickok, G., Farahbod, H., & Saberi, K. (2015). The rhythm of perception:
853 entrainment to acoustic rhythms induces subsequent perceptual oscillation.
854 *Psychological Science*, 26(7), 1006-1013.

855 Jeffreys, H. (1961). *Theory of probability* (3rd ed.). Oxford: Oxford University Press,
856 Clarendon Press.

857 Kanizsa, G. (1955). Margini quasi-percettivi in campi con stimolazione omogenea.
858 [Quasi-perceptual margins in homogeneously stimulated fields.]. *Rivista di*
859 *Psycologia*, 49, 7–30.

860 Kanizsa, G. (1979). *Organization in vision*. New York: Praeger.

861 Kass, R. E., & Raftery, A. E. (1995). Bayes factors. *Journal of the American*
862 *Statistical Association*, 90(430), 773-795.

863 Kogo, N., Strecha, C., Van Gool, L., & Wagemans, J. (2010). Surface construction by
864 a 2-D differentiation - integration process: A neurocomputational model for
865 perceived border ownership, depth, and lightness in Kanizsa figures.
866 *Psychological Review*, 117(2), 406–439.

867 Kogo, N., & Wagemans, J. (2013). The emergent property of border-ownership and
868 the perception of illusory surfaces in a dynamic hierarchical system. *Cognitive*

869 *Neuroscience*, 4(1), 54–61.

870 Kojo, I., Liinasuo, M., & Rovamo, J. (1993). Spatial and temporal properties of
871 illusory figures. *Vision Research*, 33, 897–901.

872 Lamme, V. A., & Roelfsema, P. R. (2000). The distinct modes of vision offered by
873 feedforward and recurrent processing. *Trends in Neurosciences*, 23, 571–579.

874 Lee, T. S. & Nguyen, M. (2001). Dynamics of subjective contour formation in the
875 early visual cortex. *Proceedings of the National Academy of Sciences*, 98(4),
876 1907–1911.

877 Love, J., Selker, R., Marsman, M., Jamil, T., Dropmann, D., Verhagen, A., &
878 Wagenmakers, E. J. (2015). JASP (Version 0.7)[Computer software]: Amsterdam,
879 The Netherlands: JASP Project.

880 Marr, D. (1982). *Vision*. New York: Freeman.

881 Mattingley, J. B., Davis, G., & Driver, J. (1997). Preattentive filling-in of visual
882 surfaces in parietal extinction. *Science*, 275, 671-673.

883 Michotte, A., Thines, G., & Crabbe, G. (1991). Amodal completion of perceptual
884 structures. In G. Thines, A. Costall, & G. Butterworth (Eds.), *Michotte's*
885 *experimental phenomenology of perception* (pp. 140–167). Hillsdale, NJ:
886 Erlbaum. (Original work published 1964)

887 Murray, M. M., Imber, M. L., Javitt, D. C., & Foxe, J. J. (2006). Boundary completion
888 is automatic and dissociable from shape discrimination. *The Journal of*
889 *Neuroscience*, 26(46), 12043–12054.

890 Murray, M. M., Foxe, D. M., Javitt, D. C., Foxe, J. J. (2004). Setting boundaries:
891 brain dynamics of modal and amodal illusory shape completion in humans. *The*
892 *Journal of Neuroscience*, 24, 6898-6903.

893 Neter, J., & Wasserman, W. (1974). *Applied linear statistical models*. Homewood, IL:
894 Irwin.

895 Nie, Q.-Y., Maurer, M., Müller, H. J. & Conci, M. (2016) Inhibition drives configural
896 superiority of illusory Gestalt: Combined behavioral and drift-diffusion model
897 evidence. *Cognition*, 150, 150–162.

898 Pelli, D. G. (1997). The VideoToolbox software for visual psychophysics:

899 Transforming numbers into movies. *Spatial vision*, 10(4), 437–442.

900 Pessoa, L., Thompson, E., & Noë, A. (1998). Finding out about filling-in: A guide to
901 perceptual completion for visual science and the philosophy of perception.
902 *Behavioral and Brain Sciences*, 21, 723–748.

903 Ricciardelli, P., Bonfiglioli, C., Nicoletti, R., & Umiltà, C. (2001). Focusing attention
904 on overlapping and non-overlapping figures with subjective contours.
905 *Psychological Research*, 65(2), 98–106.

906 Roelfsema, P. R., Lamme, V. A., Spekreijse, H., & Bosch, H. (2002). Figure—ground
907 segregation in a recurrent network architecture. *Journal of Cognitive*
908 *Neuroscience*, 14(4), 525–537.

909 Rogers-Ramachandran, D. C., & Ramachandran, V. S. (1998). Psychophysical
910 evidence for boundary and surface systems in human vision. *Vision Research*, 38,
911 71–77.

912 Rubin, N., Nakayama, K., & Shapley, R. (1996). Enhanced perception of illusory
913 contours in the lower versus upper visual hemifields. *Science*, 271(5249), 651.

914 Seghier, M. L., & Vuilleumier, P. (2006). Functional neuroimaging findings on the
915 human perception of illusory contours. *Neuroscience and Biobehavioral Reviews*,
916 30, 595–612.

917 Shi, Z., & Nijhawan, R. (2008). Behavioral significance of motion direction causes
918 anisotropic flash-lag and flash-mislocalization effects. *Journal of Vision*, 8(7):24,
919 1-14.

920 Shipley, T. F., & Kellman, P. J. (1992). Strength of visual interpolation depends on the
921 ratio of physically specified to total edge length. *Perception & Psychophysics*, 52,
922 97–106.

923 Shpaner, M., Molholm, S., Forde, E., & Foxe, J. J. (2013). Disambiguating the roles
924 of area V1 and the lateral occipital complex (LOC) in contour integration.
925 *Neuroimage*, 69, 146-156.

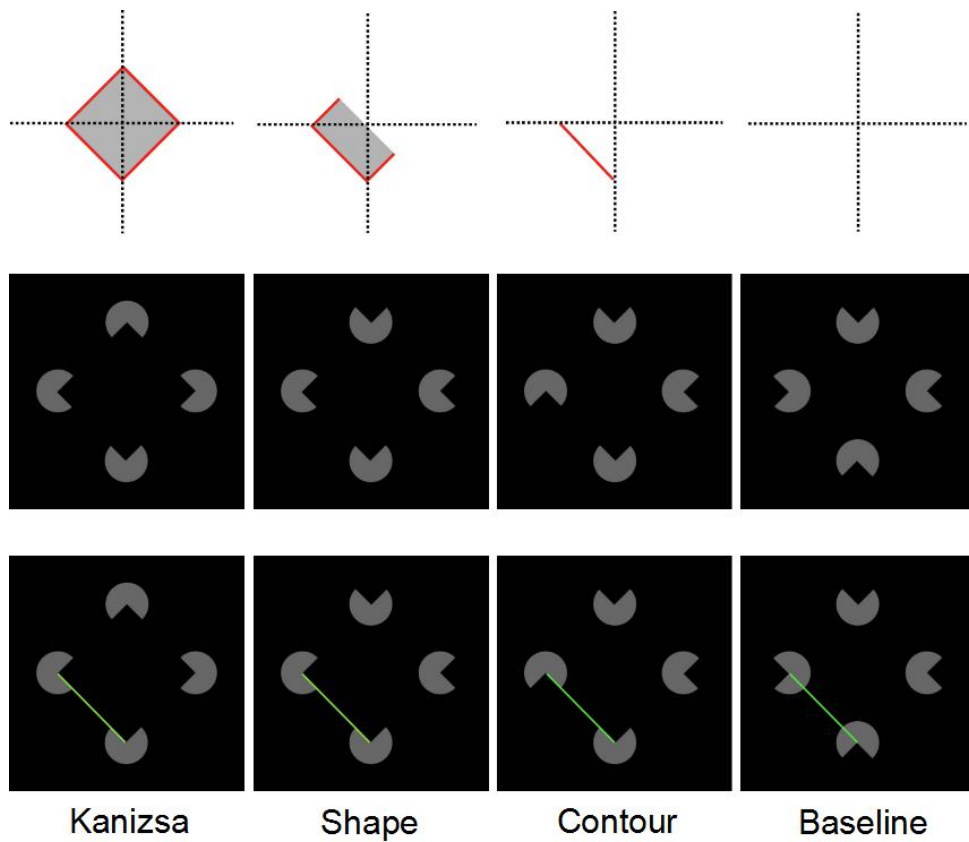
926 Shpaner, M., Stanley, D. A., Rubin, N., & Foxe, J. J. (2004). High-density electrical
927 mapping reveals early temporal differences in contour-and region-based
928 segmentation processes. *Society for Neuroscience Abstracts* (Vol. 30, No. 664.5).

- 929 Stanley, D. A., & Rubin, N. (2003). fMRI activation in response to illusory contours
930 and salient regions in the human Lateral Occipital Complex. *Neuron*, *37*(2),
931 323–331.
- 932 Van Lier, R. (1999). Investigating global effects in visual occlusion: From a partly
933 occluded square to the back of a tree trunk. *Acta Psychologica*, *102*, 203–220.
- 934 Von Der Heydt, R., Peterhans, E., & Baurngartner, G. (1984). Illusory contours and
935 cortical neuron responses. *Science*, *224*, 1260–1262.
- 936 Vuilleumier, P., & Landis, T. (1998). Illusory contours and spatial neglect.
937 *NeuroReport*, *9*(11), 2481–2484.
- 938 Vuilleumier, P., Valenza, N., & Landis, T. (2001). Explicit and implicit perception of
939 illusory contours in unilateral spatial neglect: behavioural and anatomical
940 correlates of preattentive grouping mechanisms. *Neuropsychologia*, *39*(6),
941 597–610.
- 942 Watanabe, T., & Oyama, T. (1988). Are illusory contours a cause or a consequence of
943 apparent differences in brightness and depth in the Kanizsa square? *Perception*,
944 *17*, 513–521.

945

Figures and Table

946



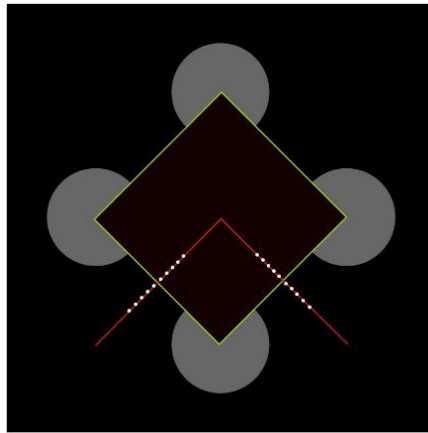
947

948

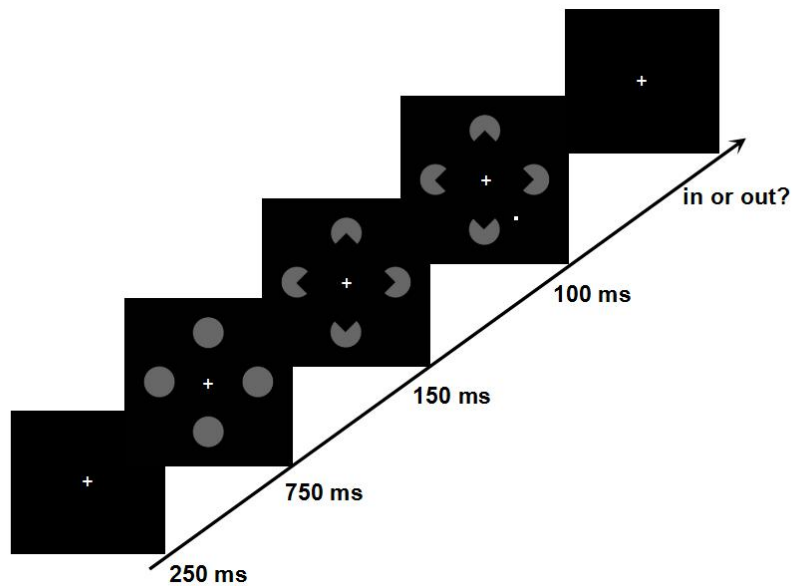
949 Figure 1. Examples of the modal completion stimuli used in Experiment 1. An
950 example of each possible configuration (Kanizsa, Shape, Contour, Baseline) is
951 depicted in the middle panels. In the examples, partial groupings in the Shape and
952 Contour stimuli are induced in the bottom-left quadrants of a given configuration. The
953 top panels illustrate the corresponding emergent grouping, displaying the respective
954 surface (gray) and contour (red) completion. In addition, the bottom panels illustrate
955 the presumed boundary of the inner region for a given configuration (green line) when
956 the dot appeared on the left side. Note that the green line was not shown in the actual
957 experiment, but only serves to illustrate the respective borders. See text for further
958 details.

959

A.

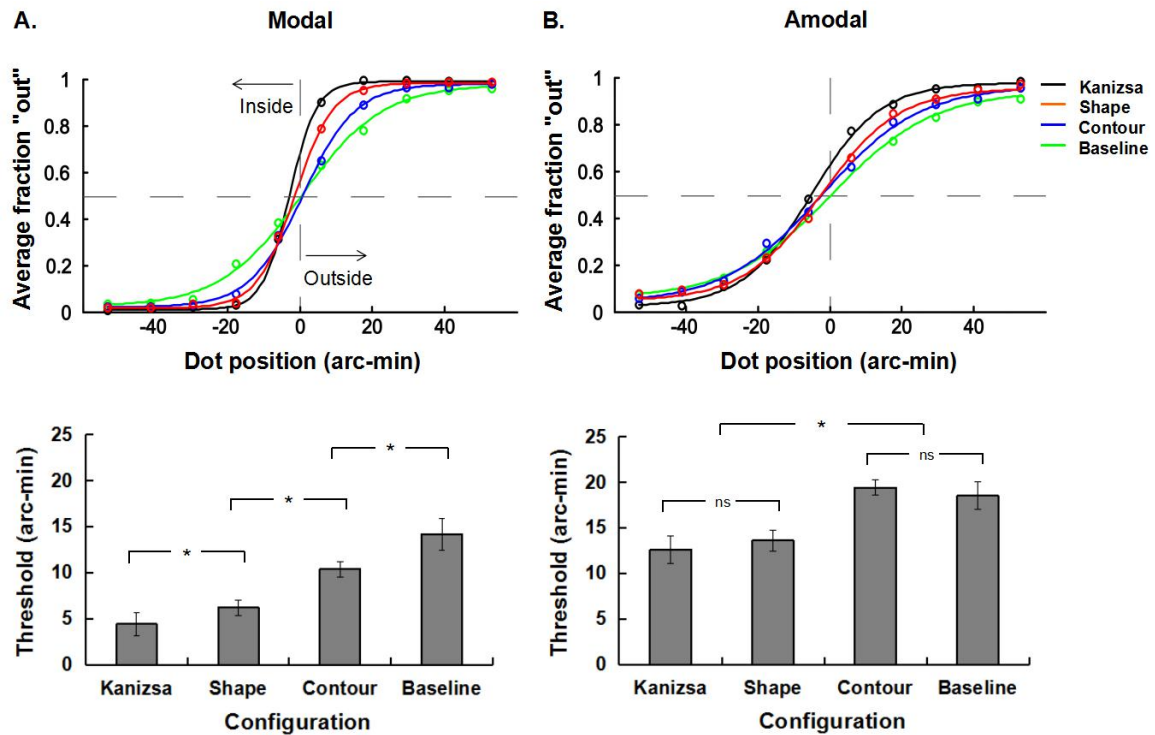


B.



960

961 Figure 2. (A) Illustration of possible dot locations in the experiments. The dot probe
962 appeared at one of ten equidistant locations along the midline (red) perpendicular to
963 the bottom left or right border (green) of the illusory figure. Note that the red and
964 green lines were not shown in the actual experiment; they only serve to illustrate the
965 stimulus layout. (B) Example trial sequence in the dot-localization task. Subsequent to
966 a pre-cue display (750 ms), a configuration display (either Kanizsa, Shape, Contour,
967 or Baseline) was briefly presented (150 ms), after which a dot probe was added and
968 presented for another 100 ms. In the example, the dot is presented near the bottom
969 right boundary of the enclosed region. Observers were instructed to report whether the
970 dot appeared inside or outside the enclosed illusory region. In the example, the correct
971 response would be ‘out’.



972

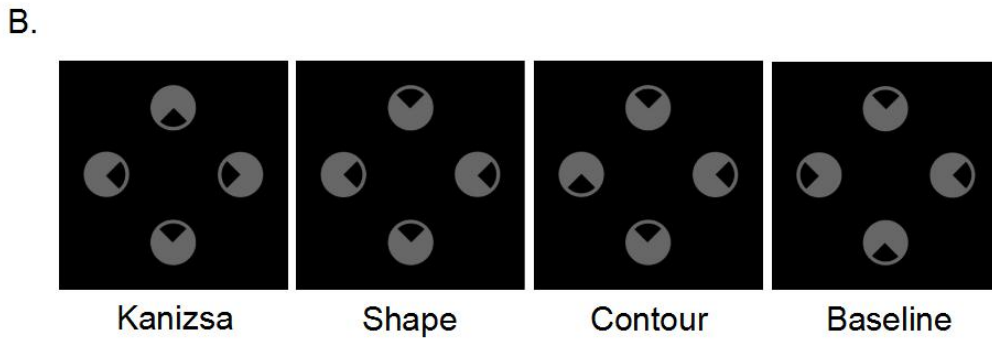
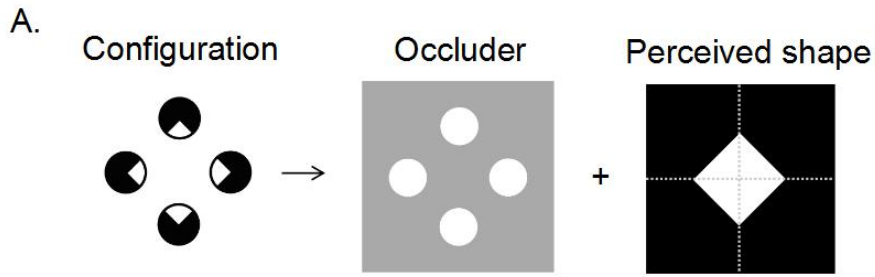
973 Figure 3. Upper panel: Psychometric curves in the dot-localization task, across
 974 observer means, in Experiment 1 (A) and Experiment 2 (B). In the graphs shown, the
 975 fraction of 'out' responses is plotted against dot position, for the Kanizsa, Shape,
 976 Contour, and Baseline conditions in the modal (A) and amodal (B) configurations.

977 Steeper slopes indicate perception of a sharper illusory figure. Note that positive
 978 values on the x-axis indicate "outside" dot-locations and negative values "inside"

979 locations. Lower panel: Corresponding mean discrimination thresholds in the Kanizsa,
 980 Shape, Contour, and Baseline conditions in Experiment 1 (A) and Experiment 2 (B).

981 Error bars denote 95% within-subject confidence intervals. * $p < .05$, Bonferroni
 982 corrected.

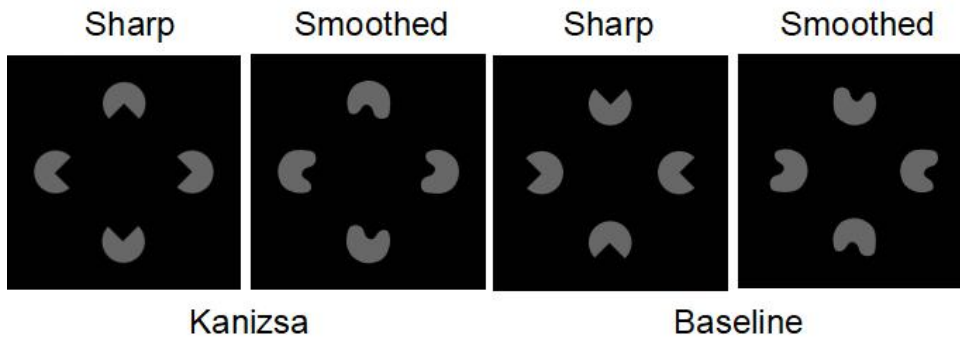
983



984

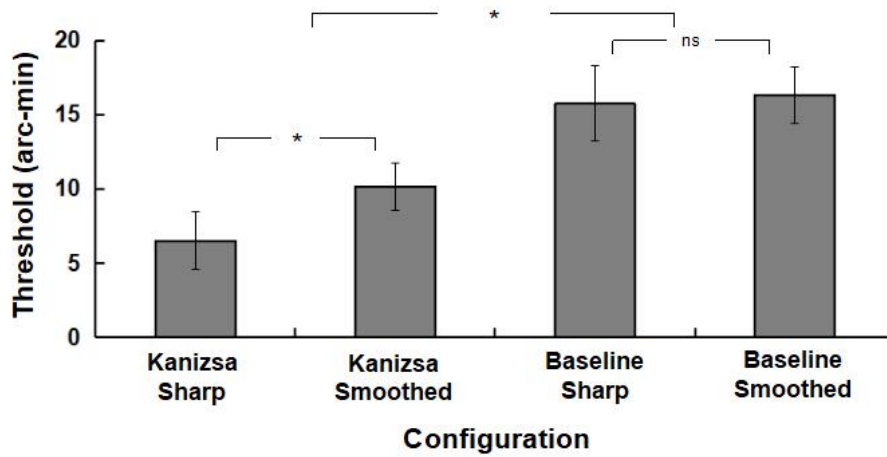
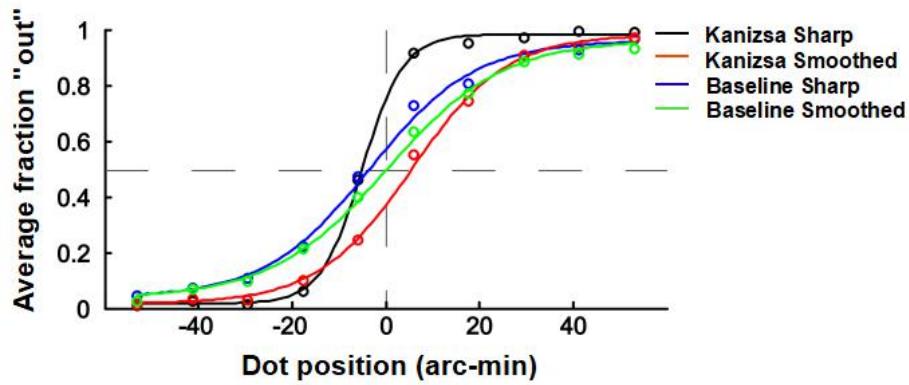
985 Figure 4. (A) An example configuration that leads to amodal completion. In the
 986 configuration, a diamond shape is perceived as lying behind an occluding surface. (B)
 987 Examples of the amodal completion stimuli used in Experiment 2. Partial groupings
 988 in the Shape and Contour stimuli are induced in the bottom-left quadrants of a given
 989 configuration.

990

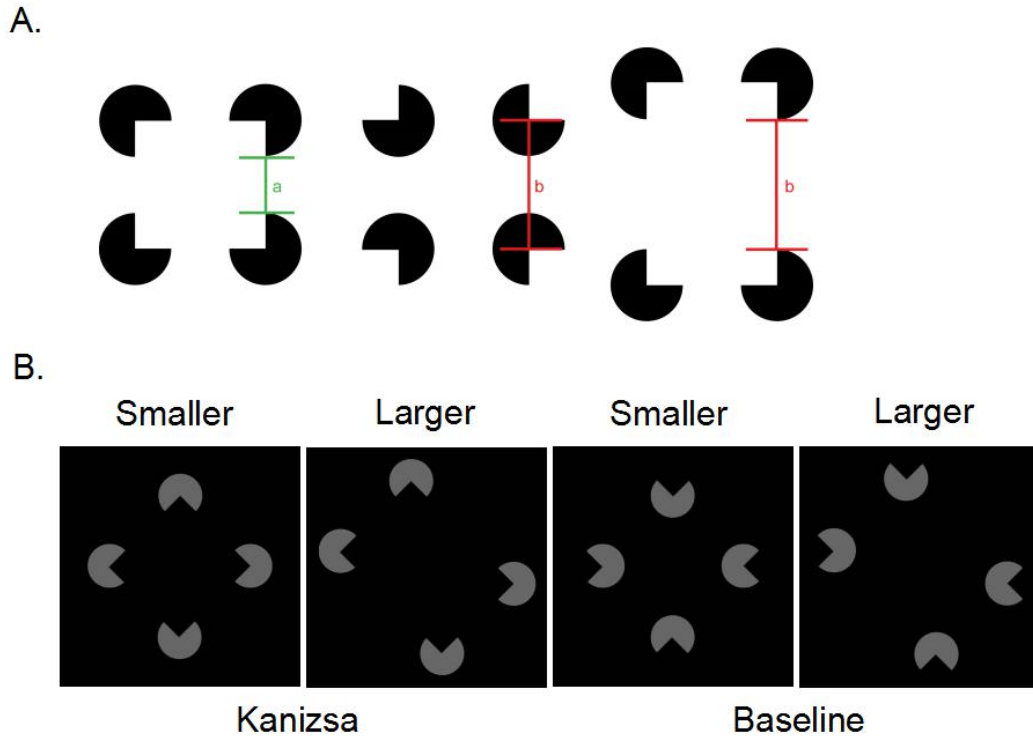


991

992 Figure 5. Example stimuli used in Experiment 3. The Kanizsa and Baseline
 993 configurations with sharp edges are the same as in Experiment 1. In the Kanizsa
 994 configuration with smoothed edges, the arrangement of the inducing elements creates
 995 an impression of an enclosed “salient” region, but this region is not bounded by crisp
 996 illusory contours.



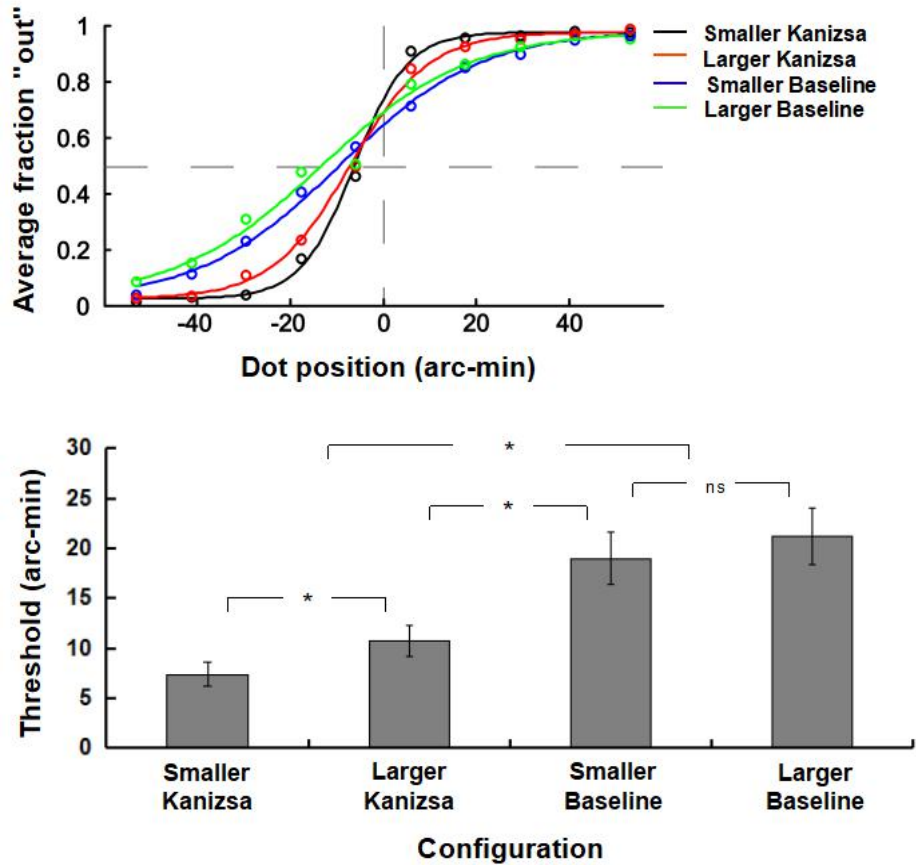
997
 998 Figure 6. Upper panel: Psychometric curves in the dot-localization task, across
 999 observer means, in Experiment 3. The fraction of ‘out’ responses is plotted against dot
 1000 position, for the Kanizsa and Baseline configurations with sharp or smoothed edges.
 1001 Lower panel: Mean discrimination thresholds in the Kanizsa and Baseline
 1002 configurations with sharp/smoothed edges in Experiment 3. Error bars denote 95%
 1003 within-subject confidence intervals. * $p < .05$, Bonferroni corrected.



1004

1005 Figure 7. (A) Variations in spatial distance across the edges of the (smaller) Kanizsa
 1006 (left panel, a) and (smaller) Baseline (middle panel, b) configurations. In the larger
 1007 Kanizsa configuration (right panel), the edge length is comparable to the smaller
 1008 Baseline configuration. (B) Example stimuli in Experiment 4. The smaller Kanizsa
 1009 and Baseline configurations were the same as in Experiment 1.

1010



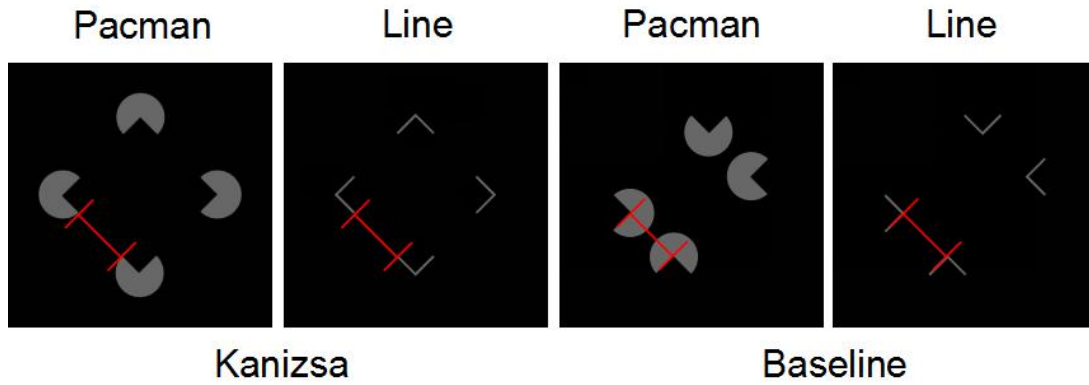
1011

1012 Figure 8. Upper panel: Psychometric curves in the dot-localization task, across
 1013 observer means, in Experiment 4. The fraction of ‘out’ responses is plotted against dot
 1014 position, for the smaller Kanizsa, larger Kanizsa, smaller Baseline, and larger
 1015 Baseline conditions. Lower panel: Mean discrimination thresholds in the smaller
 1016 Kanizsa, larger Kanizsa, smaller Baseline, and larger Baseline conditions in
 1017 Experiment 4. Error bars denote 95% within-subject confidence intervals. * $p < .05$,
 1018 Bonferroni corrected.

1019

1020

1021



1022

1023

1024

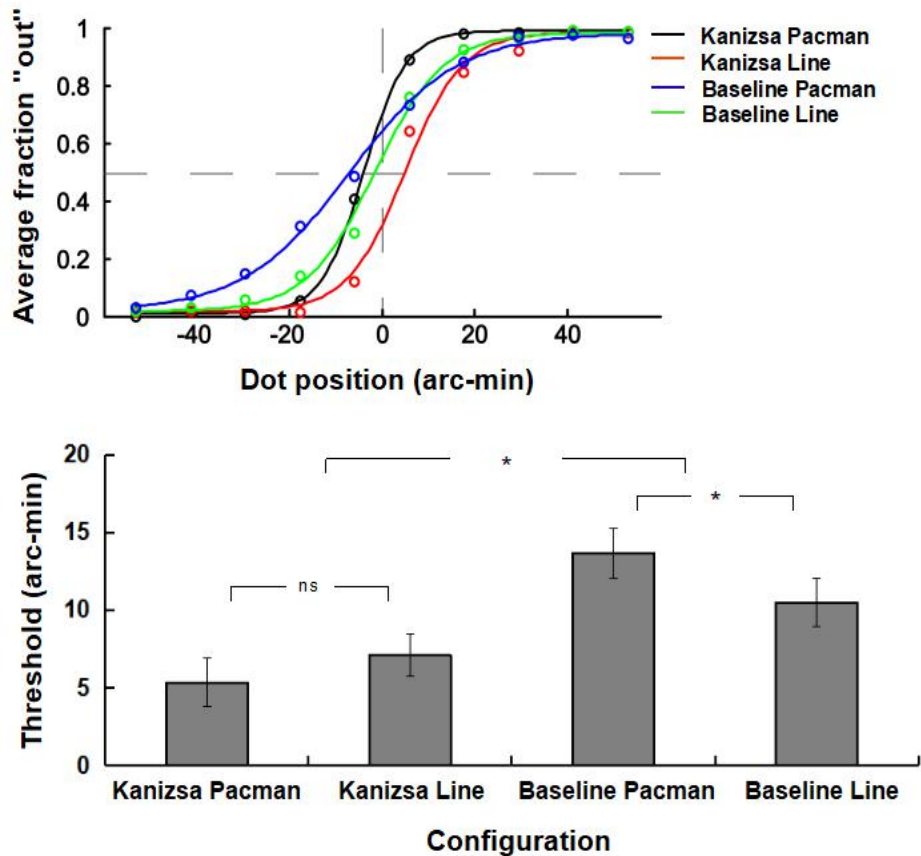
1025

1026

1027

1028

Figure 9. Example stimuli in Experiment 5, with variations of the inducer type in Kanizsa and Baseline configurations. In the Baseline configurations with pacman and line inducers, the edge length on the side where the dot appears is comparable to that in the respective Kanizsa configurations (see red lines; the line did not appear in the actual experiment). The Kanizsa figure was the same as in Experiment 1.



1029

1030 Figure 10. Upper panel: Psychometric curves in the dot-localization task, across
 1031 observer means, in Experiment 5. The fraction of ‘out’ responses is plotted against dot
 1032 position, for the Kanizsa and Baseline configurations, separately for pacman and line
 1033 inducers. Lower panel: Mean discrimination thresholds in the Kanizsa and Baseline
 1034 configurations with pacman/line inducers in Experiment 5. Error bars denote 95%
 1035 within-subject confidence intervals. * $p < .05$, Bonferroni corrected.